

A Spatial Model of Land Surface Temperature Based on the Integration of Satellite Data and IoT Sensors for Urban Heat Island Mitigation in the Climate Village Program Banjarmasin

Isna Syaunqiah^{1,*}, Ahmad Jauhari², Mufidah², Munsyi³

¹Chemical Engineering Study Program, Faculty of Engineering, Lambung Mangkurat University, Indonesia

²Department of Forestry Science, Faculty of Forestry, Lambung Mangkurat University, Indonesia

³Faculty of Da'wah and Communication Science, Universitas Islam Negeri Antasari, Indonesia

Received July 14, 2025; Revised October 20, 2025; Accepted November 19, 2025

Cite This Paper in the Following Citation Styles

(a): [1] Isna Syaunqiah, Ahmad Jauhari, Mufidah, Munsyi, "A Spatial Model of Land Surface Temperature Based on the Integration of Satellite Data and IoT Sensors for Urban Heat Island Mitigation in the Climate Village Program Banjarmasin," *Environment and Ecology Research*, Vol. 13, No. 6, pp. 797 - 807, 2025. DOI: 10.13189/eer.2025.130604.

(b): Isna Syaunqiah, Ahmad Jauhari, Mufidah, Munsyi (2025). A Spatial Model of Land Surface Temperature Based on the Integration of Satellite Data and IoT Sensors for Urban Heat Island Mitigation in the Climate Village Program Banjarmasin. *Environment and Ecology Research*, 13(6), 797 - 807. DOI: 10.13189/eer.2025.130604.

Copyright©2025 by authors, all rights reserved. Authors agree that this article remains permanently open access under the terms of the Creative Commons Attribution License 4.0 International License

Abstract The study investigates the linear regression relationship between urban IoT sensor temperatures and satellite-derived land surface temperatures (LST) to predict the effects of the Urban Heat Island (UHI) phenomenon. Satellite data from Landsat 9, combined with real-time IoT sensor data, facilitates the analysis of urban temperature variations across Banjarmasin, South Kalimantan. The regression analysis, using a model based on IoT and satellite temperature data, computes the regression coefficient and intercept, providing an equation for temperature prediction. The coefficient of determination (R^2) is employed to evaluate the model's explanatory power, revealing that 95.17% of the temperature variation can be explained by satellite data. The high R^2 value indicates a strong correlation between urban and rural temperatures. Furthermore, the Root Mean Square Error (RMSE) was calculated to quantify the prediction accuracy, yielding an RMSE of 0.714 °C, which suggests the model's high reliability. The findings demonstrate that satellite data can significantly enhance UHI mitigation strategies by informing decisions on green infrastructure implementation. The integration of IoT and satellite data offers a scalable solution for urban planners to better

address the UHI effect and improve urban resilience to climate change. The study underscores the importance of combining technological tools for more accurate and efficient climate action planning in urban areas.

Keywords Urban Heat Island, Linear Regression, Satellite Temperature, IoT Sensors, R^2 Analysis

1. Introduction

Urbanization has significantly transformed the global landscape, giving rise to various environmental challenges that require immediate attention. One of the most pressing issues is the Urban Heat Island (UHI) phenomenon [1], [2], [3]. UHI refers to the increased temperatures observed in urban areas compared to their rural counterparts, primarily due to human activities such as industrialization, deforestation, and the development of infrastructure that retain heat [4], [5]. Materials like concrete, asphalt, and steel absorb heat during the day and release it at night, causing urban areas to remain warmer than surrounding

rural regions [6]. In rapidly growing urban areas, such as Banjarmasin, the UHI effect is becoming more pronounced, with urban temperatures consistently exceeding those in nearby green spaces. Urban expansion typically leads to the reduction of vegetated areas, which are crucial for regulating local temperatures [7], [8]. The loss of vegetation exacerbates the UHI effect, negatively affecting the quality of life for urban residents. The widespread use of heat-absorbing materials and the depletion of green spaces significantly contribute to this rise in surface temperatures in large cities [9], [10]. This phenomenon results in a range of negative outcomes, including higher energy consumption for cooling, worsened air quality, and adverse effects on public health [11]. Addressing this issue requires a comprehensive, multidimensional approach that includes environmental planning, community participation, and the use of modern technologies. Technologies such as remote sensing and Internet of Things (IoT) sensors play a vital role in this context, enabling real-time monitoring and mapping of surface temperatures across urban areas affected by UHI [8]. These technologies are crucial for creating spatial models that can guide effective UHI mitigation strategies.

Recent research in Indonesia has also emphasized the importance of studying UHI from multiple perspectives, including environmental, social, and technological approaches [12]. For example, studies in Jakarta and Surabaya have reported significant LST differences between urban cores and surrounding areas, with indicators such as NDVI, Normalized Difference Built-up Index (NDBI), and albedo being frequently used to analyze spatial variations [13], [14]. Remote sensing methods, particularly with Landsat and MODIS datasets, have been widely applied to detect thermal anomalies, while ground-based sensor networks provide complementary near-surface data. Methodologies such as time-series analysis, regression models, and spatial correlation techniques further strengthen the understanding of the temporal and spatial dynamics of UHI in Indonesian cities. These findings highlight the urgent need for sustainable urban planning that integrates vegetation restoration, optimized land use, and advanced monitoring systems to mitigate UHI impacts at the city scale.

A key component in addressing the UHI effect is the integration of environmental programs, like the Climate Village Program (ProKlim) initiated by the Indonesian government [8]. ProKlim is a community-based initiative aimed at combating climate change by promoting green infrastructure, expanding vegetation, and advocating for sustainable urban planning. By involving local communities, ProKlim empowers residents to actively reduce the impacts of climate change through initiatives that enhance green spaces, restore ecological balance, and improve urban resilience to climate variability. Increasing vegetation within and around urban areas is one of the most effective methods for mitigating the UHI effect, as it can

significantly lower surface temperatures [15]. Vegetation not only provides shade, cooling the environment, but also acts as a natural carbon sink, reducing greenhouse gas emissions [16], [17]. ProKlim emphasizes collective community action, encouraging local participation in activities such as tree planting and the management of urban green spaces. The use of advanced technologies, like remote sensing and IoT sensors, enables urban planners and environmental scientists to develop detailed spatial models that track temperature variations across different zones of a city with greater accuracy [18]. These technologies facilitate more precise monitoring of land surface temperatures (LST) and provide valuable insights into areas most affected by UHI. Satellite data, combined with real-time data from IoT sensors, enables the identification of regions that need urgent intervention, such as increasing green areas or reducing the use of heat-absorbing materials [19]. Additionally, ProKlim promotes the reduction of emissions through improved waste management, energy efficiency, and the use of renewable energy sources. By incorporating these approaches, ProKlim offers a comprehensive solution for mitigating UHI and addressing broader climate change impacts in urban areas.

Remote sensing and spatial analysis are crucial in providing a deeper understanding of the environmental dynamics in urban areas, particularly in relation to UHI [20], [21]. Remote sensing technologies, including satellite platforms like Landsat 9 and Sentinel-2, are used to capture land surface temperature (LST) data and map temperature variations across urban landscapes, which are then integrated with real-time data from IoT sensors to obtain more accurate and granular temperature measurements, and to develop spatial models that guide urban heat mitigation in cities such as Banjarmasin where UHI effects are increasingly severe; in these models, the relationship between vegetation density and surface temperatures becomes explicit—areas with higher vegetation typically exhibit lower temperatures than those dominated by concrete and asphalt—thereby helping planners identify priority interventions such as tree planting or the creation of new green spaces, as well as aligning actions within the Climate Village Program to enhance resilience to broader climate challenges; the contribution and novelty of this approach lie in fusing high-spatial-resolution satellite LST with high-temporal-resolution IoT telemetry, enabling cross-calibration between satellite LST and nearby sensors via locally trained correction models, joint geospatial modeling with vegetation indicators to quantify UHI sensitivity to green cover at the neighborhood scale, and real-time hotspot detection using adaptive thresholds that update with incoming data, so that diurnal/seasonal uncertainties are better accommodated as sensor time series bridge satellite gaps; practically, this supports an operational decision dashboard linking LST and NDVI maps with live sensor streams to prioritize shading and

greening along heat-stressed corridors and residential pockets, and to evaluate impact by comparing post-intervention LST changes against nearby air-temperature traces ultimately allowing cities to implement more proactive, effective, and scalable policies that align urban development with environmental sustainability and public well-being, and that can be replicated in other cities facing similar urbanization and climate-change pressures.

2. Materials and Methods

This research employs a quantitative approach to test hypotheses using statistical calculations. Several types of analyses are utilized, including cross-tabulation, spatial regression, NDVI analysis, LST analysis, UHI analysis, sensor analysis, and spatial analysis integration of Remote Sensing and Geographic Information Systems (GIS) to support spatial modeling. The study focuses on developing a spatial UHI model for the Climate Village Program (Proklim), which involves vegetation inventory, satellite imagery (Landsat 9 and Sentinel-2) to monitor land cover changes and temperature variations, model development using field data, real-time monitoring based on IoT sensors, and satellite imagery, and validation of the model's accuracy. The model aims to provide actionable data to manage and mitigate UHI effects by enhancing vegetation in urban areas. The following methodology details the data collection, integration, and spatial analysis used to develop the UHI model, enhancing our understanding of urban temperature variations and how to address UHI through targeted interventions.

2.1. Data Collection and Preprocessing

In the initial stage of the study, satellite imagery was collected from Landsat 9 and Sentinel-2 to derive Land Surface Temperature (LST) and vegetation coverage through the Normalized Difference Vegetation Index (NDVI). These two datasets provide crucial insights into the UHI phenomenon, where LST indicates surface temperature variations, and NDVI offers information about the health and distribution of vegetation that can mitigate the UHI effect.

To calculate LST, thermal infrared data obtained from Landsat 9 [22] and Sentinel-2 were utilized. LST is computed using the formula:

$$LST = \frac{Tb}{1 + (0.0015 * \frac{Tb}{1.438}) \ln(Ep)} - 273.15 \quad (1)$$

Where Tb refers to the brightness temperature measured from the satellite's thermal infrared bands (such as Band 10 for Landsat 9). The emissivity Ep is a measure of the

surface's ability to emit radiation and is a crucial factor in adjusting the raw thermal data to account for atmospheric conditions. The formula above is used to transform the brightness temperature into an accurate surface temperature in degrees Celsius. This transformation is necessary to eliminate the effects of atmospheric interference, such as water vapor and air molecules, which may distort the satellite data.

The NDVI, which helps assess the density and health of vegetation, was calculated using the near-infrared (NIR) and red bands of the satellites [23]. The formula for NDVI is:

$$NDVI = \frac{NIR-RED}{NIR+RED} \quad (2)$$

Where:

NIR is the near-infrared band from Sentinel-2

RED is the red band from Sentinel-2

The NDVI ranges from -1 to 1, with values closer to 1 indicating healthy, dense vegetation, and values closer to -1 indicating barren land or water. Areas with higher NDVI values are likely to have cooling effects due to the evapotranspiration process of plants, which helps counteract the UHI effect [24].

Once LST and NDVI values were calculated, the satellite images were further processed for cloud masking, using algorithms that identified and removed clouds and cloud shadows from the images. This step is essential as clouds and their shadows can obscure the true surface temperatures and vegetation indices, leading to inaccuracies in the results. The data were then clipped to the area of interest, which in this study was the urban zones of Banjarmasin, South Kalimantan, Indonesia.

The preprocessing of satellite data involved not only the application of these calculations, but also ensuring the quality and accuracy of the data by applying radiometric and geometric corrections. These corrections were necessary to remove errors related to sensor calibration and to align the satellite imagery with the Earth's coordinate system. The result was a set of high-quality, spatially accurate data that could then be used for further analysis.

2.2. Integration of IoT Data

IoT sensors were deployed across various urban zones, focusing on areas prone to experiencing high Urban Heat Island (UHI) effects. IoT technology allows for real-time environmental monitoring, providing more granular and timely data than satellite observations, which are limited by revisit times and cloud cover. The primary advantage of IoT is its ability to continuously monitor temperature, humidity, and soil moisture at specific locations, which is essential for a dynamic and accurate representation of temperature variation in urban environments [25].

IoT sensors are strategically placed in urban areas with varying levels of vegetation cover. These nodes were equipped with sensors to measure both air and soil temperature, providing continuous data that could be integrated with satellite-based temperature data for validation and accuracy enhancement. To combine this real-time data with satellite-based LST, linear regression analysis was used to correlate the two datasets [26]. The linear regression model is expressed as:

$$y = \alpha X + b \quad (3)$$

where:

y is the dependent variable (IoT data),

X is the independent variable (satellite data),

α is the regression coefficient (slope),

b is the intercept (constant).

The integration of IoT data also allowed for the identification of specific microclimates within urban environments that were susceptible to higher temperatures, which satellite imagery alone could not capture due to its lower temporal resolution. The IoT system also helped identify temperature variations that occurred during different times of the day, including nighttime, when the UHI effect is most pronounced. This dynamic data allows urban planners to devise more targeted interventions, such as increasing green space or optimizing urban surfaces to reflect more sunlight, thereby mitigating UHI.

2.3. Spatial Modeling and Analysis

The integration of both IoT data and satellite-derived information was used to develop a spatial model to map UHI intensity across the urban area. To facilitate spatial modeling, Google Earth Engine (GEE) was employed as the platform for analyzing the combined datasets. GEE provides powerful tools for spatial data processing, enabling the combination of IoT real-time data with satellite imagery and performing spatial analysis efficiently [27].

One key technique used in this spatial analysis is Kriging, a geostatistical interpolation method that estimates the value of a variable at unmeasured locations based on values at surrounding locations. Kriging is especially useful for filling in the gaps where IoT data is not available, and for creating a smooth, continuous spatial map of temperature variation across the urban environment [28]. The Kriging interpolation formula is as follows:

$$Z(u) = \sum_{i=1}^n Z\lambda_i(x_i) \quad (4)$$

where:

$Z(u)$ is the estimated temperature at location u ,

$Z(x_i)$ is the observed temperature at location x_i ,

λ_i are the weights determined by the spatial distance and covariance between points.

The weights λ_i are calculated by solving the spatial covariance matrix, which ensures that closer observations contribute more to the estimate than those farther away. The spatial covariance function measures how much two points in space are correlated based on their distance from each other.

Kriging allows the generation of high-resolution temperature maps, enabling the identification of UHI hotspots within the urban environment. These maps can then be used by urban planners and local governments to target areas that require interventions, such as increasing urban green spaces, adding reflective surfaces, or introducing cooling technologies in high-temperature areas.

In addition to Kriging, other spatial analysis techniques were applied, including regression analysis and spatial autocorrelation, to understand the relationship between UHI intensity and urban factors such as land use, population density, and vegetation cover. These analyses revealed that areas with lower NDVI values (indicating less vegetation) consistently experienced higher surface temperatures, supporting the hypothesis that increasing vegetation can effectively reduce UHI.

Furthermore, the spatial model was validated by comparing predicted temperatures from the model with actual IoT measurements using statistical metrics such as Root Mean Square Error (RMSE). The RMSE was calculated using the formula:

$$RMSE = \sqrt{\frac{1}{n} \sum (y_i - \bar{y})^2} \quad (5)$$

y_i represents the observed temperature at point i ,

\bar{y} represents the predicted temperature at point i ,

n is the total number of observations.

To evaluate how well the linear regression model predicts IoT air temperatures from satellite-based inputs, this study reports the coefficient of determination, R^2 . Conceptually, R^2 represents the proportion of total variability in the observed urban temperature that is explained by the model's predictions derived from the satellite (rural) temperature. Values range from 0 to 1, where values closer to 1 indicate that the model captures the data pattern with smaller residual errors. Prior to computing R^2 , the dataset was time-aligned and cleaned to remove outliers so that comparisons reflect consistent measurement conditions. In the context of UHI assessment, a high R^2 supports using satellite information to infer near-surface thermal conditions, and to track temporal changes in urban-rural temperature contrasts for monitoring and policy evaluation. The following equation defines R^2 using the observed temperatures, the model-predicted temperatures, and the mean of all IoT temperature observations, followed by a description of each term.

The formula used to calculate R^2 is:

$$R^2 = 1 - \frac{\sum (y_i - \bar{y}_i)^2}{\sum (y_i - \bar{y})^2} \quad (6)$$

where:

y_i is the actual temperature value measured by IoT (Urban),

\bar{y}_i is the temperature value predicted by the linear regression model based on Satellite temperature (Rural),

\bar{y} is the average of all IoT temperature values.

2.4. Region of Interest

The region of interest encompasses the administrative extent of Banjarmasin, the capital of South Kalimantan, situated on a low-lying deltaic plain at the confluence of the Barito and Martapura rivers, and bordered by Barito Kuala Regency to the north until west and Banjar Regency to the south until east. The city is segmented into

five districts: North, West, Central, East, and South, each intersected by dense road networks and a fine hydrological mesh of rivers and canals that shape local microclimates and urban morphology. Central Banjarmasin functions as the urban core with high built-up density, flanked by mixed residential-commercial zones in the West and North, while larger patches of open water and vegetated land are more prevalent toward the South and East, offering clear contrasts in land cover needed to examine NDVI-LST relationships and UHI gradients. Given the city's flat topography, tidal influence, and humid tropical rainfall regime, the ROI is well suited for multi-season analysis that differentiates dry and wet season thermal patterns, supports peridistrict aggregation of indicators, and aligns with policy frameworks such as community-based climate action and green-infrastructure targeting. The following Figure 1 is an administrative map of Banjarmasin.

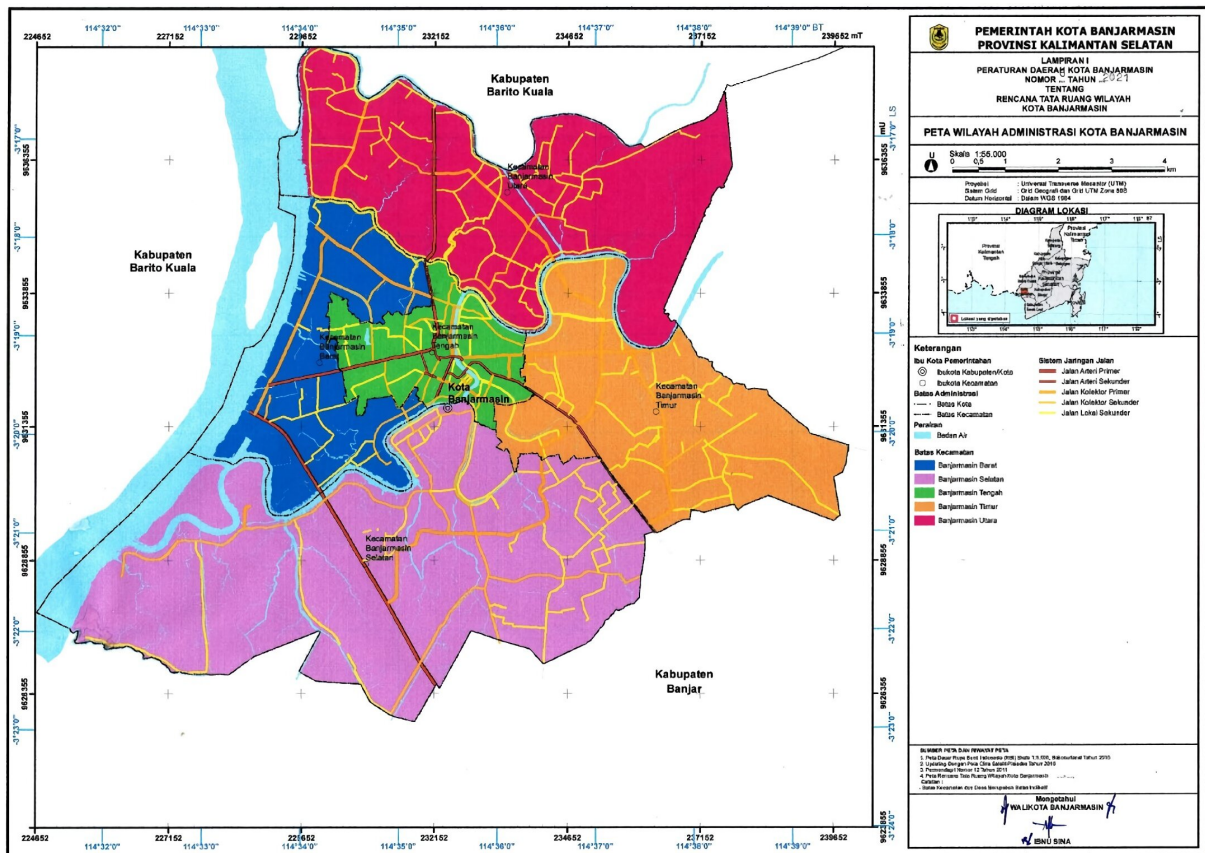


Figure 1. Administrative map of Banjarmasin City

3. Results and Discussion

In this study, we analyzed LST data in South Kalimantan using GEE. The analysis revealed significant variations in LST across different areas, providing valuable insights into the UHI phenomenon in the region of Climate village Program Banjarmasin, with the coordinates [114.60164316191577, -3.296326363850163]. Based on the data obtained, LST in Climate village Program Banjarmasin City showed minimum and maximum values, reflecting the temperature differences between urban and rural areas. The minimum LST values were recorded in areas with denser vegetation cover, while the maximum LST values were observed in highly urbanized areas.

The LST map for Climate Village Program Banjarmasin in Figure 2, South Kalimantan, from 2024 reveals significant temperature variations across the region, with temperatures ranging from approximately 20.59 °C in cooler areas (depicted in blue) to 30.87 °C in warmer areas (shown in red). The map employs a color scale to highlight these temperature differences, offering crucial insights into the spatial distribution of heat within the city. Urbanized zones, especially around the city center, exhibit higher temperatures, which is characteristic of the UHI effect. These areas, marked in yellow and red, are typically made up of concrete, asphalt, and other materials that absorb and retain heat, leading to significant temperature increases compared to surrounding rural areas. Conversely, the cooler areas, mostly along the riverbanks and regions with dense vegetation, are marked in blue. These areas benefit from the natural cooling effects of vegetation, which provides shade and promotes

evapotranspiration, a process that cools the surrounding environment. The UHI effect is particularly evident in the city center, where temperatures are significantly higher due to human activities, infrastructure, and heat retention by built surfaces. The UHI intensity in Banjarmasin ranges from -3.93 °C to 1.24 °C, with the highest UHI values found in the urban core. This variation illustrates the stark contrast in temperature between the urban areas and their rural surroundings, exacerbated by the absorption of heat in urbanized zones. The LST and UHI data provide essential information for urban planners, highlighting the need for strategies to mitigate the UHI effect. Implementing more green spaces, promoting sustainable urban planning, and using reflective materials in infrastructure could help reduce the urban heat buildup and enhance the overall environmental quality. The understanding serves as a basis for further research and initiatives aimed at improving the city's resilience to climate change while fostering a healthier and more sustainable urban environment. Understanding the seasonal dynamics of vegetation cover can help guide urban planning, agricultural management, and conservation efforts, so areas with low vegetation can be prioritized for restoration or reforestation projects. Additionally, monitoring NDVI trends can help identify areas at risk of environmental degradation, enabling timely interventions to mitigate the impacts of climate change and urban expansion. By integrating such data into decision-making processes, cities can better align their growth strategies with environmental sustainability goals. The NDVI analysis results we studied can be seen in Figure 3.

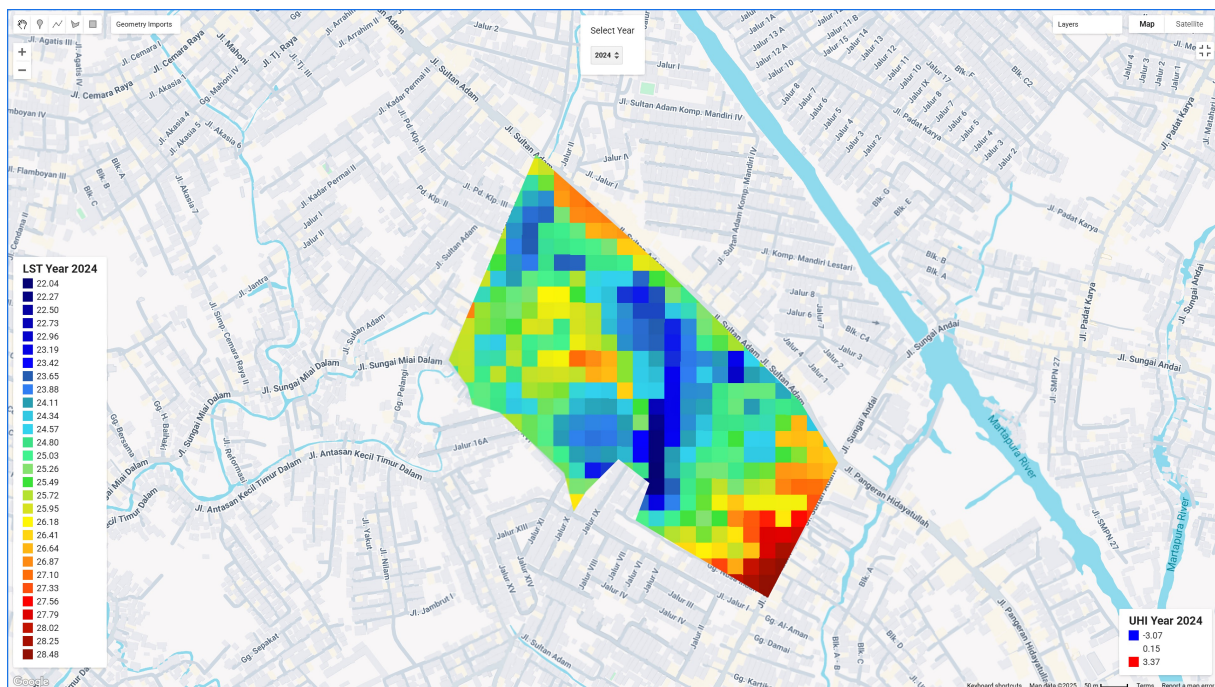


Figure 2. Analysis LST Result in Climate Village Program Banjarmasin using Landsat 9

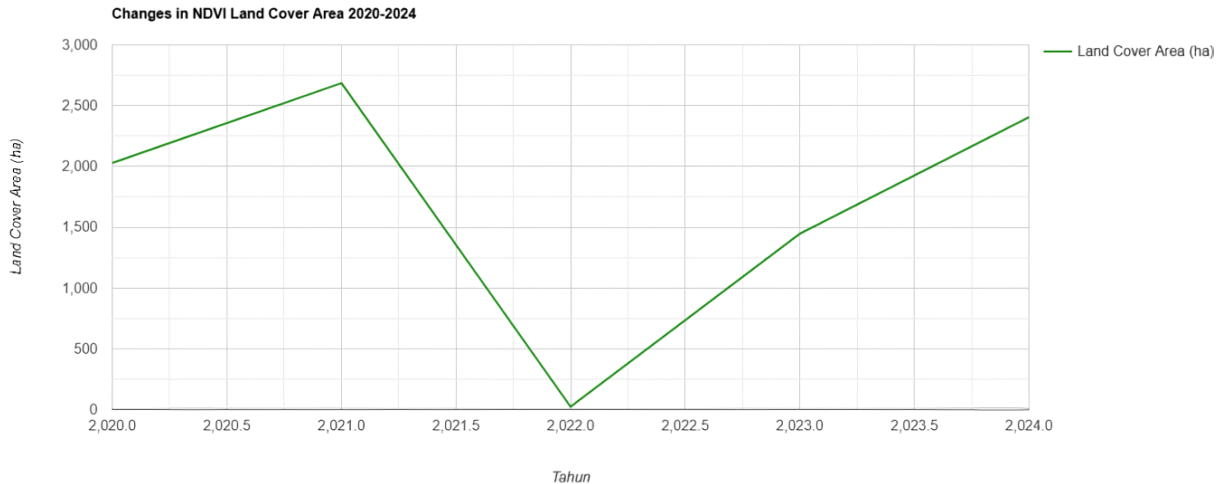


Figure 3. Land Cover Area (NDVI) Result in GEE using Sentinel-2

The NDVI-derived land cover area exhibits a clear sequence of early increase, sudden collapse, and subsequent recovery between 2020 and 2024, as traced by the green line in the figure. Starting from roughly 2,000 ha in 2020, the curve rises to about 2,700 ha in 2021, indicating a strong expansion of vegetated cover relative to the baseline year. This upward momentum abruptly reverses in 2022, when the series drops to near zero, marking an outlier year that stands in stark contrast to adjacent observations and strongly suggests either a data discontinuity or an extreme disturbance signal rather than a gradual ecological trend. The pattern then rebounds in 2023 to approximately 1,500 ha, signaling a partial restoration of vegetated area from the 2022 trough but still notably below the 2021 maximum. By 2024, the trajectory climbs further to around 2,400 ha, recovering most of the loss since 2022 and surpassing the 2020 baseline while remaining modestly below the 2021 peak. Interpreted as a multi-year profile, the sequence forms a V-shaped recovery: robust pre-2022 gains, a singular nadir in 2022, and a two-year ascent that re-establishes substantial vegetated extent by 2024. Year-to-year slopes reinforce this narrative, with a positive 2020–2021 gradient, a steep negative 2021–2022 break, and progressively positive gradients from 2022–2023 and 2023–2024. From a reporting perspective, 2022 should be annotated as an exceptional year, and trend statements should emphasize the return to high coverage levels by 2024 relative to the baseline while acknowledging the gap to the 2021 maximum. Overall, the chart communicates resilience in vegetated land cover following a transient disruption, culminating in a strong late-period recovery that positions 2024 as a near-peak outcome within the observed window.

The IoT Sensor data measurements provide additional benefits in the form of an early warning system to detect significant temperature increases in Proklim areas. The system can be accessed via mobile devices connected to the internet. The interface display of the system built is

shown in Figure 4.

In Figure 4 with real-time monitoring from IoT data, we collected the data such as air and soil temperature and humidity. Additionally, data from IoT can be integrated into spatial models to support Proklim planning. This model can be used to identify priority areas for vegetation-based interventions, and also provides a data-driven framework that can support decision-making in efforts for sustainable UHI mitigation.

To determine the linear relationship between Satellite Temperature (Rural) and IoT Temperature (Urban), we need to calculate the regression coefficient (*a*), which indicates the rate of change in urban temperature relative to changes in satellite temperature, and the intercept (*b*), which represents the starting point of urban temperature. With accurate calculations, we can obtain the regression equation that provides an estimate of IoT temperature based on satellite data, enabling predictive analysis and UHI mitigation. The calculation for the coefficient and intercept is as follows:

$$\alpha = \frac{\sum(Xi - \bar{X}) - (yi - \bar{y})}{\sum(Xi - \bar{X})^2} \tag{7}$$

From the above formula, the calculation proceeds with the following steps:

1. Calculate the average values \bar{X} and \bar{y} where the average satellite temperature is 26.15°C, and the average IoT temperature is 27.99°C.
2. Calculate the deviation from the average data by computing the deviation for each pair using the formula $\sum(Xi - \bar{X}) - (yi - \bar{y})$ and square the satellite temperature deviations using the formula $\sum(Xi - \bar{X})^2$. Using this formula, the results obtained are $a = 0.9148$ and $b = 4.0665$, where the equation used for the intercept is $b = \bar{y} - a\bar{X}$. After the calculations, the linear equation obtained is $y = 0.9148X + 4.0665$, where the data for IoT and Satellite used in the calculations can be seen in Table 1.

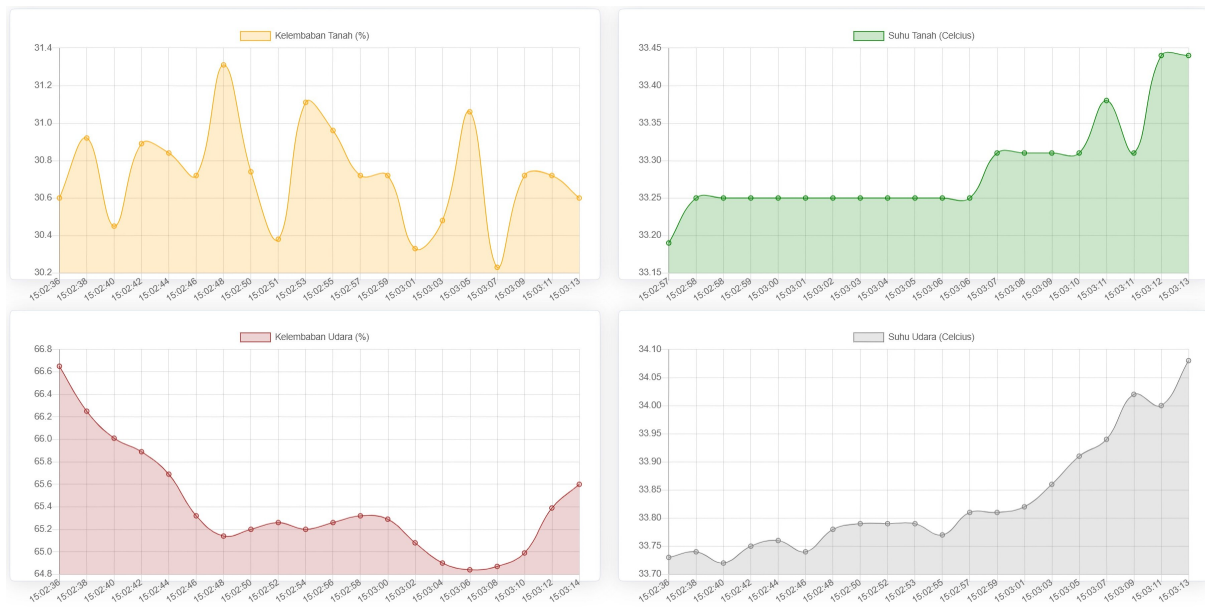


Figure 4. Real-time data from Internet of Things

Table 1. Comparison of Satellite and IoT Data

Num.	Date	IoT Data	Satellite Data
1	12/27/2023	22,31	19,18
2	01/01/2024	22,34	21,18
3	01/18/2024	26,66	25,24
4	02/12/2024	27,33	25,36
5	02/28/2024	30,88	27,89
6	03/14/2024	31,03	28,06
7	04/12/2024	28,89	25,24
8	04/29/2024	27,92	25,36
9	05/14/2024	29,21	27,89
10	05/30/2024	28,88	27,06
11	06/22/2024	30,11	27,22
12	07/12/2024	29,21	26,99
13	07/30/2024	30,23	27,01
14	08/09/2024	31,21	28,02
15	08/18/2024	30,22	28,09
16	09/19/2024	34,21	31,02
17	09/26/2024	32,87	31,09
18	10/28/2024	24,33	29,51
19	11/08/2024	24,22	26,05
20	11/24/2024	25,33	23,13
21	12/08/2024	24,29	22,09
22	12/24/2024	23,87	22,41

To assess how well the linear regression model explains the relationship between Satellite Temperature (Rural) and IoT Temperature (Urban), the coefficient of determination (R^2) is used. The R^2 value indicates the percentage of variation in IoT temperature data that can be explained by Satellite temperature, with values ranging from 0 to 1. The closer the value is to 1, the better the model explains the relationship between the two variables. By calculating R^2 , we can evaluate whether the linear regression model used is sufficiently accurate or needs further improvement by considering other factors.

The calculation results show that the obtained R^2 value is 0.9517, indicating that 95.17% of the variation in IoT temperature data can be explained by Satellite temperature. This value suggests that the linear regression model used has a high degree of accuracy in predicting urban surface temperatures based on satellite-derived temperatures. However, even though the R^2 value is close to 1, further validation is carried out using additional evaluation methods such as Root Mean Square Error (RMSE) to ensure the model's reliability under various environmental conditions.

In linear regression analysis, RMSE is used to measure

the average error between predicted values and actual values in the same units as the original data. RMSE provides insight into how far the model's predictions are from the actual values, with smaller values indicating a more accurate model in representing the relationship between Satellite (Rural) and IoT (Urban) temperatures.

After cleaning the temperature dataset from Table 1 by removing outliers, a simple linear regression was fitted to quantify the relationship between rural (satellite-derived) temperature and urban (IoT-measured) surface temperature. Figure 5 plots each observation as a blue cross, with satellite temperature on the x-axis ($^{\circ}\text{C}$) and IoT urban temperature on the y-axis ($^{\circ}\text{C}$), and overlays the red regression line that summarizes the overall upward trend. The updated model explains most of the variation in urban temperature ($R^2=0.9517$) and has a small typical prediction error (RMSE = 0.714), showing that satellite temperature can accurately predict IoT temperature within the observed range. In practical terms, for any satellite temperature value in the figure's domain, the regression line provides the corresponding predicted urban temperature, while the vertical spread of points around the line indicates the remaining uncertainty.

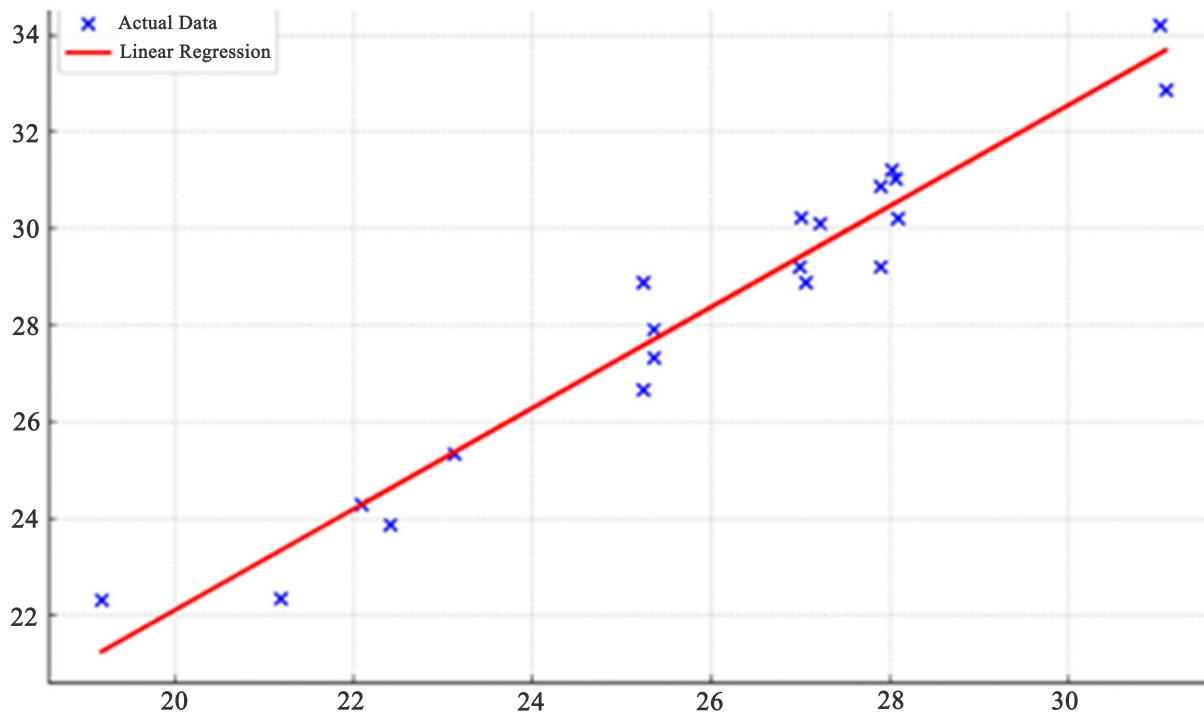


Figure 5. Linear Regression Analysis of Urban Temperature vs. Rural Temperature

4. Conclusions

The integration of IoT sensors and satellite-derived temperature data provides a robust method for understanding and addressing the Urban Heat Island (UHI) effect. The linear regression model used in this study effectively correlates IoT and satellite data, with a high R^2 value of 0.9517, indicating that satellite temperature data can predict urban surface temperatures with high accuracy. The RMSE value of 0.714 °C further supports the reliability of the model. This research highlights the potential of combining real-time IoT data and satellite imagery to develop spatial models for UHI mitigation. By identifying areas with high UHI intensity, urban planners can target interventions such as increasing green spaces, using reflective materials, or optimizing urban layouts to reduce surface temperatures, thus improving urban resilience to climate change and promoting a healthier environment. Future research should refine the spatial models by incorporating additional environmental variables such as humidity and air quality, expanding the use of IoT sensors in diverse urban areas, and integrating data from different satellite platforms to enhance accuracy. Further studies should also explore the long-term impact of vegetation-based interventions on UHI mitigation to assess their sustainability. Lastly, these models should be extended to other cities with varying climates to evaluate their scalability and adaptability in different urban environments.

Acknowledgements

The authors would like to express their sincere gratitude to the Directorate of Research and Community Service (Direktorat Penelitian dan Pengabdian kepada Masyarakat – DPPM), Ministry of Education, Culture, Research, and Technology (Kemendikbudristek), for providing research funding through the 2025 Regular Fundamental Research Scheme under the contract number: Induk Contract No. 075/C3/DT.05.00/PL/2025.

REFERENCES

- [1] B. Alahmad, L. P. Tomasso, A. Al-Hemoud, P. James, and P. Koutrakis, "Spatial distribution of land surface temperatures in Kuwait: Urban heat and cool Islands," *Int. J. Environ. Res. Public Health*, vol. 17, no. 9, pp. 1–11, 2020, doi: 10.3390/ijerph17092993.
- [2] N. da Silva Espinoza *et al.*, "Assessment of urban heat islands and thermal discomfort in the Amazonia biome in Brazil: A case study of Manaus city," *Build. Environ.*, vol. 227, p. 109772, 2022, doi:10.1016/j.buildenv.2022.109772.
- [3] S. Kandel, B. Gyawali, J. Sandifer, S. Shrestha, and S. Upadhaya, "Assessment of Urban Heat Islands (UHIs) Using Satellite-Derived Normalized Difference Vegetation Index (NDVI), and Land Surface Temperature (LST) in Three Metropolitan Cities of Nepal," *Banko Janakari*, vol. 32, no. 2, pp. 37–51, 2022, doi: 10.3126/banko.v32i2.50895.
- [4] Z. S. Han *et al.*, "Observed sea breeze life cycle in and around NYC: Impacts on UHI and ozone patterns," *Urban Clim.*, vol. 42, p. 101109, 2022, doi: 10.1016/j.uclim.2022.101109.
- [5] M. Pena Acosta, M. Dikkers, F. Vahdatikhaki, J. Santos, and A. G. Dorée, "A comprehensive generalizability assessment of data-driven Urban Heat Island (UHI) models," *Sustain. Cities Soc.*, vol. 96, p. 104701, 2023, doi: 10.1016/j.scs.2023.104701.
- [6] S. Jain, S. Sannigrahi, S. Sen, S. Bhatt, S. Chakraborti, and S. Rahmat, "Urban heat island intensity and its mitigation strategies in the fast-growing urban area," *J. Urban Manag.*, vol. 9, no. 1, pp. 54–66, 2020, doi: 10.1016/j.jum.2019.09.004.
- [7] L. Taati, Sunardi, I. Syauqiah, and A. Jauhari, "Assessing Drought Risk in Forest Zones Near Coal Mines with Temperature Vegetation Dryness Index," *J. Appl. Data Sci.*, vol. 5, no. 2, pp. 559–570, 2024, doi: 10.47738/jads.v5i2.20.
- [8] Munsyi, A. Nugroho, A. Jauhari, and M. R. Faisal, "Urban Heat Island Spatial Model for Climate Village Program Planning," *J. Appl. Data Sci.*, vol. 5, no. 2, pp. 546–558, 2024, doi: 10.47738/jads.v5i2.223.
- [9] A. A. Scott, D. W. Waugh, and B. F. Zaitchik, "Reduced Urban Heat Island intensity under warmer conditions," *Environ. Res. Lett.*, vol. 13, no. 6, 2018, doi: 10.1088/1748-9326/aabd6c.
- [10] H. D. Nirwana, A. R. Saidy, G. M. Hatta, and A. Nugroho, "Design of a Green City with Lower Carbon Based on Vegetation in Banjarbaru using Sentinel-2," *J. Appl. Data Sci.*, vol. 5, no. 2, pp. 583–599, 2024, doi: 10.47738/jads.v5i2.218.
- [11] H. Ashraf, T. A. El Seoud, S. Sodoudi, and A. El Zafarany, "Anisotropic Surface Urban Heat Island in Cairo, Egypt: A Spatiotemporal Analysis of Local Climate Change from 2000 to 2021," *Civ. Eng. Archit.*, vol. 11, no. 1, pp. 331–350, 2023, doi: 10.13189/cea.2023.110127.
- [12] N. Nandi and M. Dede, "Urban Heat Island Assessment using Remote Sensing Data in West Java, Indonesia: From Literature Review to Experiments and Analyses," *Indones. J. Sci. Technol.*, vol. 7, no. 1, pp. 105–116, 2022, doi: 10.17509/ijost.v7i1.44146.
- [13] A. Saputra, M. H. Ibrahim, S. Shofirun, A. Saifuddin, and K. Furoida, "Assessing Urban Heat Island in Jakarta, Indonesia During the Pandemic of Covid-19," *Iop Conf. Ser. Earth Environ. Sci.*, vol. 986, no. 1, p. 12069, 2022, doi: 10.1088/1755-1315/986/1/012069.
- [14] Rivan Aji Wahyu Dyan Syafitri, Adjie Pamungkas, and Eko Budi Santoso, "The Impact of Urban Configuration to the Urban Heat Island in East Surabaya," *IPTEK J. Proc. Ser.*, no. 6, 2020, doi: 10.12962/j23546026.y2020i6.11145.
- [15] Z. Muttaqin, A. Yulianti, and K. Karmanah, "Climate village program (ProKlim) in Simurugul Sub-Village, Margawati Village, Garut Kota Sub-Regency, Garut

- Regency, West Java Province, Indonesia,” *IOP Conf. Ser. Earth Environ. Sci.*, vol. 299, no. 1, 2019, doi: 10.1088/1755-1315/299/1/012046.
- [16] U. Gessner, S. Reinermann, S. Asam, and C. Kuenzer, “Vegetation Stress Monitor—Assessment of Drought and Temperature-Related Effects on Vegetation in Germany Analyzing MODIS Time Series over 23 Years,” *Remote Sens.*, vol. 15, no. 22, 2023, doi: 10.3390/rs15225428.
- [17] L. Safitri, M. Galdos, A. Challinor, and A. Comber, “The relationship between spatial variation of greenhouse gases intensity and agri-environmental variables in Oil Palm plantations,” EGU General Assembly 2023, Vienna, Austria, 24–28 Apr 2023, EGU23-14986, 2024, doi: 10.5194/egusphere-egu23-14986.
- [18] Munsiy, A. Sudarsono, and M. U. H. Al Rasyid, “Secure Data Exchange Based on Wireless Sensor Network for Environmental Monitoring Using Dynamical Attributed Based Encryption,” *Int. J. Adv. Sci. Eng. Inf. Technol.*, vol. 11, no. 4, pp. 1306–1315, 2021, doi: 10.18517/ijaseit.11.4.8546.
- [19] N. Li and J. Wang, “Comprehensive Eco-Environment Quality Index Model with Spatiotemporal Characteristics,” *Sensors*, vol. 22, no. 24, 2022, doi: 10.3390/s22249635.
- [20] Bhartendu Sajan, Shruti Kanga, Suraj Kumar Singh, Varun Narayan Mishra, and Bojan Durin, “Spatial variations of LST and NDVI in Muzaffarpur district, Bihar using Google earth engine (GEE) during 1990-2020,” *J. Agrometeorol.*, vol. 25, no. 2 SE-Research Paper, pp. 262–267, May 2023, doi: 10.54386/jam.v25i2.2155.
- [21] A. Yuliawati, R. A. Pramadi, M. Zuldin, D. K. Yusuf, A. N. Jamaludin, and U. Patoni, *Recommended plants for green open space to enrich bird diversity in Gedebage region Bandung West Java*, vol. 1098, no. 5. 2021. doi: 10.1088/1757-899x/1098/5/052002.
- [22] E. Abdul Kadir, S. Listia Rosa, A. Syukur, M. Othman, and H. Daud, “Forest fire spreading and carbon concentration identification in tropical region Indonesia,” *Alexandria Eng. J.*, vol. 61, no. 2, pp. 1551–1561, 2022, doi: 10.1016/j.aej.2021.06.064.
- [23] A. Grover and R. B. Singh, “Analysis of urban heat island (Uhi) in relation to normalized difference vegetation index (ndvi): A comparative study of delhi and mumbai,” *Environ. - MDPI*, vol. 2, no. 2, pp. 125–138, 2015, doi: 10.3390/environments2020125.
- [24] S. Guha, H. Govil, and P. Diwan, “Monitoring LST-NDVI Relationship Using Premonsoon Landsat Datasets,” *Adv. Meteorol.*, 2020, doi: 10.1155/2020/4539684.
- [25] S. Navulur, A. S. C. S. Sastry, and M. N. Giri Prasad, “Agricultural management through wireless sensors and internet of things,” *Int. J. Electr. Comput. Eng.*, vol. 7, no. 6, pp. 3492–3499, 2017, doi: 10.11591/ijece.v7i6.pp3492-3499.
- [26] Munsiy, A. Sudarsono, and M. U. H. Al Rasyid, “Secure Data Sensor In Environmental Monitoring System Using Attribute-Based Encryption With Revocation,” *Int. J. Adv. Sci. Eng. Inf. Technol.*, vol. 7, no. 2, p. 609, 2017, doi: 10.18517/ijaseit.7.2.2175.
- [27] K. Onáčillová, M. Gallay, D. Paluba, A. Péliová, O. Tokarčík, and D. Laubertová, “Combining Landsat 8 and Sentinel-2 Data in Google Earth Engine to Derive Higher Resolution Land Surface Temperature Maps in Urban Environment,” *Remote Sens.*, vol. 14, no. 16, 2022, doi: 10.3390/rs14164076.
- [28] D. A. Enquobahrie *et al.*, “Prenatal exposure to particulate matter and placental gene expression,” *Environ. Int.*, vol. 165, p. 107310, 2022, doi: 10.1016/j.envint.2022.107310.